This is a repository copy of *Hif-1alpha stabilisation is protective against infection in zebrafish comorbid models*.

White Rose Research Online URL for this paper:
http://eprints.whiterose.ac.uk/162036/

Version: Published Version

Article:

eprints@whiterose.ac.uk
https://eprints.whiterose.ac.uk/

Hif-1alpha stabilisation is protective against infection in zebrafish comorbid models

Yves Schild[1,2,3], Abdirizak Mohamed[1,2], Edward J. Wootton[1,2], Amy Lewis[1,2] and
Philip M. Elks[1,2]

1 The Bateson Centre, University of Sheffield, Sheffield, UK
2 Department of Infection, Immunity and Cardiovascular Disease, University of Sheffield, Sheffield, UK
3 Universität Duisburg Essen, Duisburg, Germany

Multi-drug-resistant tuberculosis is a worldwide problem, and there is an urgent need for host-derived therapeutic targets, circumventing emerging drug resistance. We have previously shown that hypoxia-inducible factor-1α (Hif-1α) stabilisation helps the host to clear mycobacterial infection via neutrophil activation. However, Hif-1α stabilisation has also been implicated in chronic inflammatory diseases caused by prolonged neutrophilic inflammation. Comorbid infection and inflammation can be found together in disease settings, and it remains unclear whether Hif-1α stabilisation would be beneficial in a holistic disease setting. Here, we set out to understand the effects of Hif-1α on neutrophil behaviour in a comorbid setting by combining two well-characterised *in vivo* zebrafish models – TB infection (*Mycobacterium marinum* infection) and sterile injury (tailfin transection). Using a local Mm infection near to the tailfin wound site caused neutrophil migration between the two sites that was reduced during Hif-1α stabilisation. During systemic Mm infection, wounding leads to increased infection burden, but the protective effect of Hif-1α stabilisation remains. Our data indicate that Hif-1α stabilisation alters neutrophil migration dynamics between comorbid sites and that the protective effect of Hif-1α against Mm is maintained in the presence of inflammation, highlighting its potential as a host-derived target against TB infection.

Introduction

Multi-drug resistance is an increasing problem worldwide, and in 2017, World Health Organization (WHO) estimated that there were 490 000 cases of multi-drug-resistant *Mycobacterium tuberculosis* infections [the bacterial pathogen that causes tuberculosis (TB)], alongside 600 000 new cases with resistance to the front-line drug rifampicin [1]. There is an urgent and unmet need for host-derived therapeutic targets that

would circumvent the problems of emerging drug resistance and could work in combination with current antimicrobials to completely clear patients of TB burden more rapidly [2].

Neutrophil activation can be viewed as a double-edged sword during disease, with pathogen elimination being beneficial to the host while surrounding tissue damage caused by excessive neutrophil inflammation

Abbreviations

CFU, colony-forming unit; CHT, caudal haematopoietic tissue; COPD, chronic obstructive pulmonary disease; DA Hif-1α, dominant active Hif-1α; DMOG, dimethyloxalylglycine; DMSO, dimethyl sulfoxide; dpf, days post fertilisation; dpi, days post infection; GPCRs, G protein-coupled receptors; Hif-1α, hypoxia-inducible factor-1alpha; HIV, human immunodeficiency virus; HK, heat-killed; hpf, hours post infection; hpw, hours post wound; Mm, *Mycobacterium* marinum; mpc, minutes post-(photo)conversion; Mtb, *Mycobacterium* tuberculosis; NI, not injected; PR, phenol red; PVP, polyvinylpyrrolidone; TB, tuberculosis; WHO, World Health Organization.

bringing negative outcomes [3]. Neutrophils must distinguish between sterile and infected tissue injuries to determine an appropriate response [4], one that strikes a balance between infection control and tissue damage, but the mechanisms behind this are not well understood in complex *in vivo* tissue environments, partially due to a lack of appropriate models. Damage-associated molecular patterns and pathogen-associated molecular patterns share some receptor repertoires and downstream signalling components, but there is evidence to suggest that neutrophils can differentiate between these signals [5].

Neutrophils are involved early in TB infection with influx associated with killing of bacteria in a number of cellular and animal models [3,6–8], but their function during mycobacterial infection is not well characterised. Neutrophils are important in infection control; however, they are also the drivers of many chronic inflammatory diseases such as chronic obstructive pulmonary disease (COPD) [9]. Neutrophils are one of the first immune cell types to respond to tissue injury and migrate to the wound to clear fragments of dead cells and protect against pathogen invasion [10]. However, in order for wounds to heal, neutrophilic inflammation must resolve, either by programmed cell death (apoptosis), or by movement away from the wound in a process called reverse migration [11,12]. If neutrophils persist, then excessive degranulation, alongside more recently described neutrophil extracellular traps, leads to build-up of toxic components and tissue damage, causing further neutrophil recruitment, a vicious cycle of chronic inflammation that underpins many inflammatory diseases like COPD [13,14].

Chronic diseases, such as TB and COPD, often do not occur individually but exist together in patients, a situation called comorbidity. This is true of TB, as one-third of the world's population live healthily with latent TB infection for decades before a 'second-hit' comorbidity leads to progression to active TB [15]. Some of the best characterised comorbidities are co-infections with other communicable diseases, most notably human immunodeficiency virus (HIV) which causes immune deficiency and allows TB to breakout of granulomas leading to active disease [1]. However, at the same time as anti-retroviral therapy is bringing HIV under greater control, there is an alarming rise in noncommunicable diseases, such as diabetes and COPD, in the same populations that have been linked to TB activation [15,16]. Many of these noncommunicable diseases have an inflammatory component, yet treatment of these diseases, and indeed TB itself, is currently tailored towards the single condition rather than considering the holistic outcome of the

comorbidity [17]. This is reflected in animal models used to investigate cellular and molecular mechanisms of disease often being based on a single condition rather than considering comorbidities, and there is a pressing need for comorbid models to understand the complex interactions of cells in these contexts *in vivo*.

Neutrophils are exquisitely sensitive to low levels of oxygen (hypoxia), which pro-longs their lifespan and increases their bactericidal mechanisms [12,18,19]. The cellular response to hypoxia involves the activation and stabilisation of hypoxia-inducible factor-1α (HIF-1α) transcription factor [20,21]. We have previously demonstrated that activating neutrophils, via stabilisation of Hif-1α, is host protective during *in vivo* mycobacterial infection – a good therapeutic outcome [22]. However, hypoxia and Hif-1α have also been shown to delay neutrophil apoptosis and reverse migration of neutrophils away from wounds in chronic inflammation models – a bad therapeutic outcome [12,23]. Therefore, the beneficial effects of Hif-1α stabilisation on a holistic-scale during infection remain unclear, due to the potential for neutrophil damage and chronic inflammation.

The zebrafish has become an invaluable animal model for TB and inflammatory disease over the last 15 years [24]. Infection of zebrafish larvae with *Mycobacterium marinum* (Mm), a closely related strain to human Mtb and a natural fish pathogen, has been used to identify important molecular mechanisms involved in TB pathogenesis and granuloma formation [25]. Zebrafish embryos are transparent, and innate immune cell transgenic lines have been used over the last decade in tailfin transection models to better understand the molecular mechanisms involved in both neutrophil recruitment to, and reverse migration from, a site of inflammation [12,26,27].

Here, we investigated the effects of Hif-1α stabilisation on neutrophil dynamics in comorbid models of infection and wounding by combining well-characterised zebrafish Mm infection and tailfin transection models [12,22]. During systemic infection, neutrophil inflammation dynamics at the tailfin wound occur as normal while presence of a wound exacerbates infection burden. By switching to a localised infection, we show that interaction between tailfin inflammation neutrophils and the site of infection occurs and that infection can attract neutrophils away from the tailfin wound prematurely. Our data show that, on a local scale, stabilisation of Hif-1α can alter neutrophil migration dynamics, but that, on an entire organism level, the host-protective effect of Hif-1α stabilisation against infection remains. These findings demonstrate that comorbidities may have multiscale effects ranging

from the local tissue to holistic levels and that Hif-1α is a promising drug target against TB, even in the presence of an inflammatory comorbidity.

Results

Mm infection induced neutrophil emergency haematopoiesis and was increased by a comorbid wound

Infection and inflammation commonly occur in the same individual during disease, yet many *in vivo* experimental systems investigate immune responses to these processes independently of each other. We set out to develop *in vivo* zebrafish models of infection and inflammation, that we have termed 'comorbid models'. Initially, we combined two well-defined models: a Mm model of systemic infection with injection of bacteria into the caudal vein at 30–32 hours post fertilisation (hpf) that allows assessment of bacterial burden at 4 days post infection (dpi), and a tailfin wound model of neutrophilic inflammation [transection of the tailfin at 2 days post fertilisation (dpf) with neutrophil inflammation resolving at 24 hours post wound (hpw)] [27,28] (Fig. 1A).

We first assessed whether injury at the caudal vein (the site of Mm infection) caused by the microinjection process itself would affect neutrophil behaviour at the tailfin wound. Injection of polyvinylpyrrolidone (PVP) into the caudal vein (mock infection control) caused no difference to the number of neutrophils at the peak of recruitment to the tailfin wound (6 hpw), nor after neutrophil inflammation resolution at 24 hpw (not injected, NI, compared to PVP injected) (Fig. 1B).

The presence of systemic Mm infection increased neutrophil number at the wound at both the 6 and 24 hpw timepoints compared to NI and PVP controls (Fig. 1B). Although overall neutrophil numbers were increased by infection at 6 and 24 hpw (Fig. 1B), the percentage change in neutrophil number between 6 and 24 hpw remained the same across groups (Fig. 1C). We assessed whole-body neutrophil counts after Mm infection without a tailfin injury and confirmed that total neutrophil number was increased after Mm infection (Fig. 1D) consistent with emergency haematopoiesis, likely contributing to the higher neutrophil numbers observed at the wound after infection [29]. Infection levels were measured in the comorbid model using fluorescent Mm and assessing bacterial burden at 4 dpi. Levels of Mm infection were significantly increased in the presence of neutrophilic inflammation at the wound site compared to non-wounded controls (Fig. 1E) indicating that the

presence of localised tailfin inflammation is detrimental to infection control.

Local somite Mm infection lowers neutrophil numbers at the tailfin wound

To investigate neutrophil migration to infection and wound stimuli in a comorbid model, we switched from a systemic infection to a local infection challenge in order to create a single focus of infection. We challenged 3dpf zebrafish larvae with a tailfin wound immediately followed by a local somite infection into the 26–27th somite (Mm or PVP mock infection control) and counted neutrophils at each site over time. Unlike systemic infection (Fig. 1D), local somite infection did not increase whole-body neutrophil number over the 4 h post infection/wound time period of this assay (Fig. 2A,B). When challenged with Mm infection alone or tailfin wound alone, neutrophils migrated to each respective site and numbers peaked at 4–6 hpw/i (Fig. 2C–E). Of note, some neutrophils were present at the site of infection before challenge (on average 10 neutrophils) due to the natural distribution of neutrophils at this stage, with very few present at the end of the tail (the wound site, < 5 neutrophils) (Fig. 2C–E). When tailfin wounding was followed by PVP injection (as a mock infection control), neutrophils migrated to both the somite PVP site and the tailfin wound site, indicating that a wound in the somite was sufficient to attract neutrophils (Fig. 2D–E). When tailfin wounding was followed by somite Mm infection, neutrophils migrated to the somite infection site at the expense of tailfin wound neutrophils (Fig. 2C–E).

We next investigated whether neutrophils migrate from a somite wound to the tailfin wound. Photoconversion (PC) of neutrophils of *TgBAC(mpx: Gal4.VP16);Tg(UAS:Kaede)i222 (shortened to mpx: Kaede) larvae* allows fate-tracking of specific populations of neutrophils. We photoconverted neutrophils in the caudal vein region, anterior to the somite wound, and tracked their migration over 4 h post-somite infection/tailfin transection (Fig. 3A). We observed that in PVP somite injections, red neutrophils that were photoconverted in the caudal haematopoietic tissue (CHT), primarily migrate to the site of somite injection, but are not retained at this injection wound, instead migrate towards the tailfin transection wound (Fig. 3B). Conversely, when Mm was injected into the somite, the majority of photoconverted neutrophils were recruited to the infection and were retained at the site instead of migrating towards the tailfin transection (Fig. 3B–D). Over the 4-h time lapse, few neutrophils
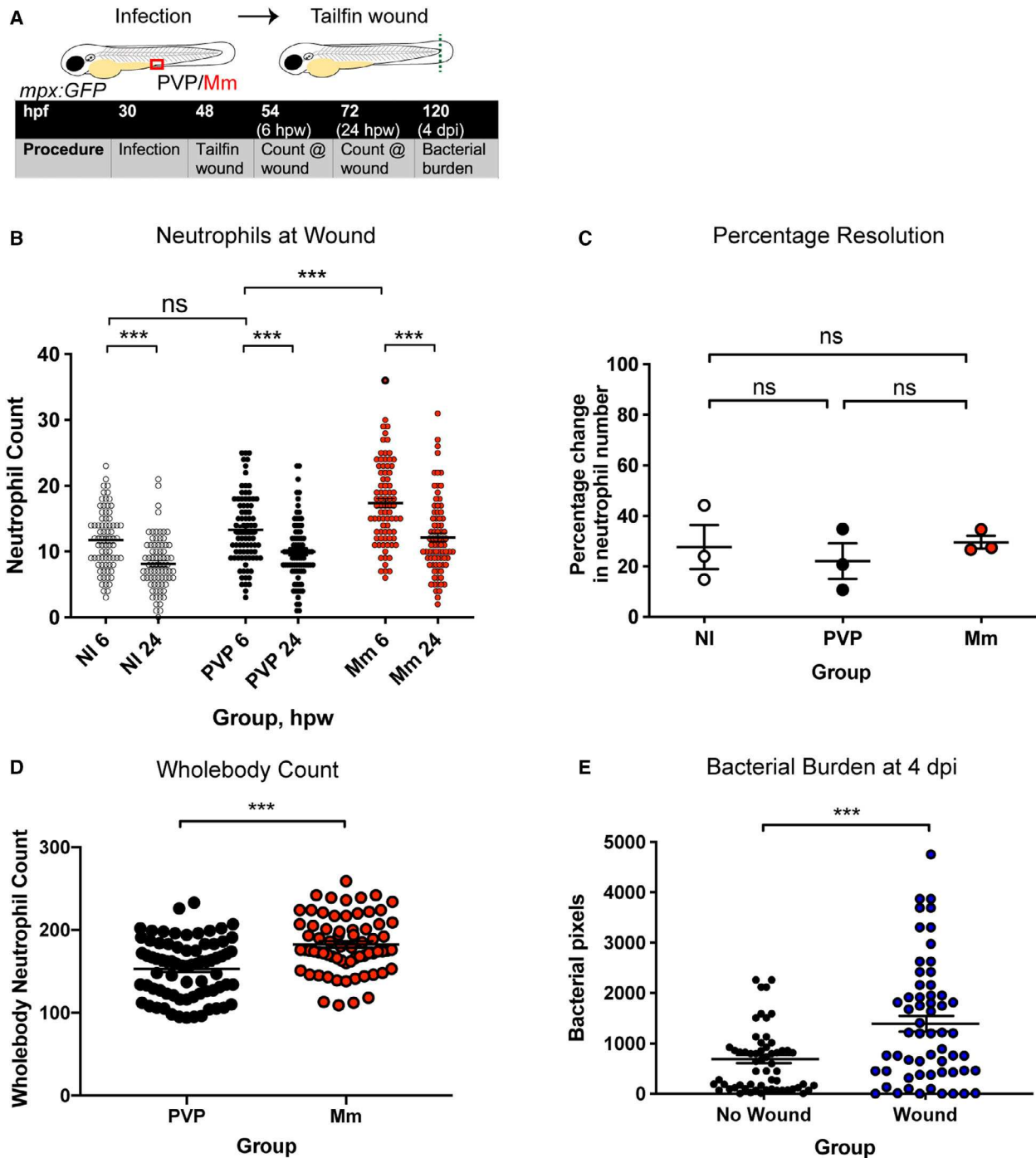
Fig. 1. Mm infection induced neutrophil emergency haematopoiesis and was increased by a comorbid wound. (A) Schematic of experiment for B, C and E. (B) Neutrophil numbers at the wound at 6 and 24 hpw of *mpx:GFP* embryos. Groups are NI, control injection with PVP and Mm injection. Data shown are mean ± SEM, n = 75–85 accumulated from three independent experiments. Statistics were determined using one-way ANOVA (with Bonferroni's multiple comparisons test). *P* values shown are as follows: ns = not significant and ***P < 0.001. (C) Percentage resolution of neutrophilic inflammation (percentage change in neutrophil number at the tailfin wound between 6 and 24 hpw). Groups are NI, control injection with PVP and Mm injection. Data shown are mean ± SEM, n = 75–85 from three independent experiments. Statistics were determined using one-way ANOVA (with Bonferroni's multiple comparisons test). *P* values shown are as follows: ns = not significant. (D) Total, whole-body neutrophil numbers at 2 dpf, after 18 hpi with PVP or Mm. Data shown are mean ± SEM, n = 69–74 accumulated from three independent experiments. Statistics were determined using an unpaired *t*-test. *P* values shown are as follows: ***P < 0.001. (E) Bacterial burden of larvae with or without a tailfin wound. Data shown are mean ± SEM, n = 58 accumulated from three independent experiments. Statistics were determined using an unpaired *t*-test. *P* values shown are as follows: ***P < 0.001.

migrated to the tailfin wound in Mm-infected larva (Fig. 3B–D), and of those that did they took a direct route to the tailfin wound, bypassing the infection (Fig. 3B, red track). Together, these data indicate that the signal gradient caused by Mm infection is additive to that of the somite injury alone and that neutrophils preferentially migrate to Mm and are retained at infection rather than travelling further along the trunk to the tailfin wound.

Finally, we examined whether the attractant effect of Mm on neutrophils was dependent on live bacteria. We used heat-killed (HK) bacteria and found that there was no statistical difference between the neutrophil number at 4hpi/w at either the somite infection or the tailfin wound compared to live Mm (Fig. 4A-D). HK Mm caused a significant increase in neutrophil numbers at infection compared to PVP-injected controls, similar to live Mm (Fig. 4C). However, the neutrophil localisation pattern of the HK Mm-infected larva appeared to be intermediate between PVP injection and live Mm (Fig. 4B), and indeed, HK Mm did not significantly decrease neutrophil numbers at the tailfin wound compared to PVP-injected controls, while live Mm did (Fig. 4D). Therefore, these data indicate that signals from HK Mm are sufficient to attract neutrophils to the site of infection, but suggest a minor contribution of the bacteria being alive to neutrophil migration behaviours in this assay.
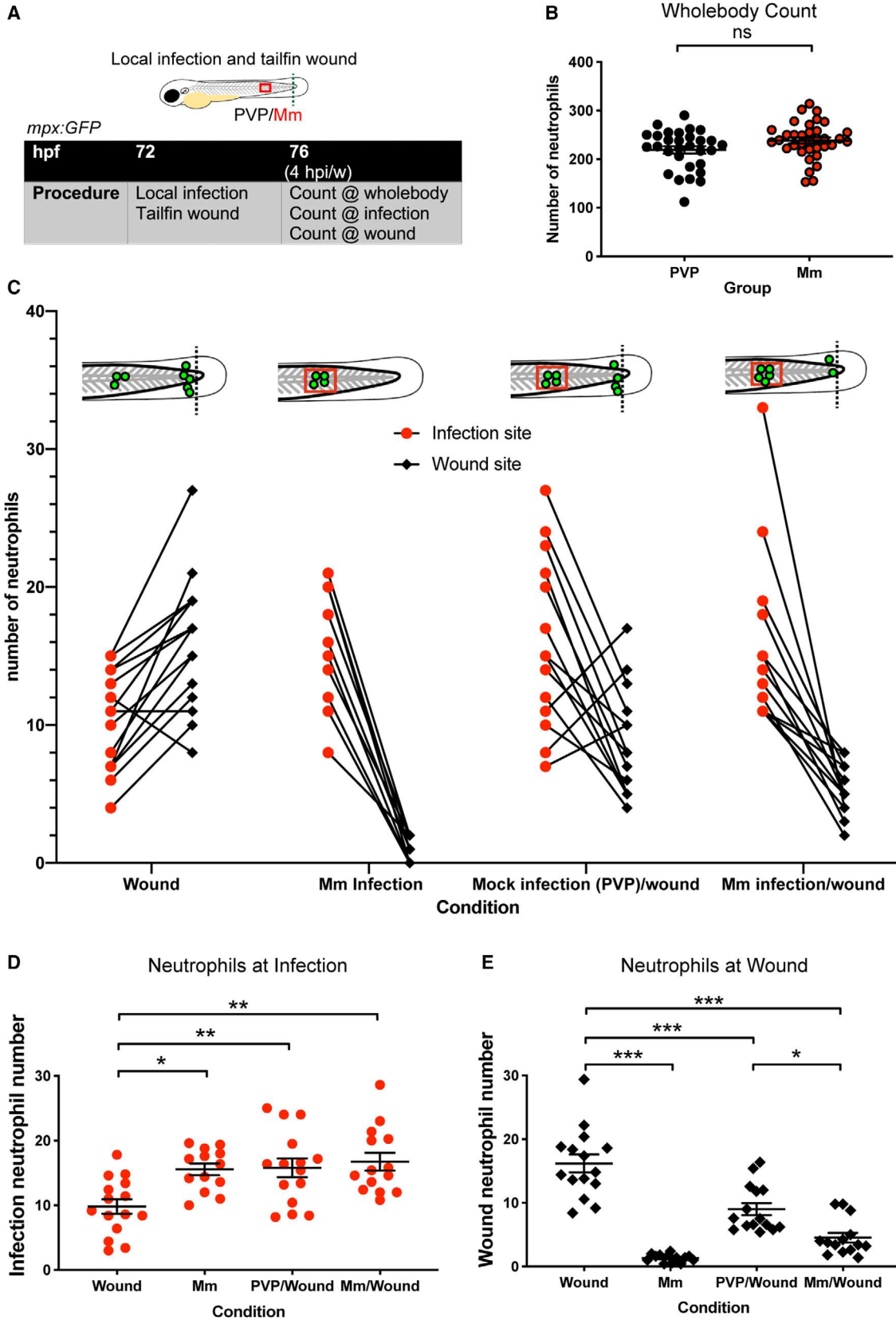
Neutrophils preferentially migrated to a new infection stimulus rather than patrol the wound site

In a single model of tailfin wound, once neutrophils have migrated to a wound site (between 1 and 6 hpw), they are retained at the wound, patrolling until the resolution phase of inflammation (6–12 hpw) [12,27]. We have previously demonstrated that neutrophils migrate away from the wound by a diffusion process at around 8–12 hpw when neutrophils become desensitised to signals that retains them at the wound [30]. We hypothesised that infection can overcome this retention signal at the wound site and attract neutrophils prematurely away from the wound. To determine whether infection can overcome retention signals and attract neutrophils away from a tailfin wound, we changed the localised infection model so that the infection challenge was performed at a time when neutrophils are present at the tailfin wound and are still being recruited. At 4 hpw, a localised Mm infection was introduced into the 26–27th somite (Fig. 5A). 4 hpw is a timepoint at which neutrophils would not have started to reverse migrate away in a single wound model, a process that

normally occurs after 6–12 hpw [10,12]. PC of *mpx: Kaede* neutrophils at the tailfin wound at 4 hpw allowed identification of neutrophils that had visited the wound ('wound-experienced' red neutrophils), compared to those that had not ('wound-naïve' green neutrophils). We demonstrated that injection of Mm into the 26–27th somite was sufficient to attract neutrophils away from the wound (wound-experienced neutrophils) between 4 and 6 hpw (Fig. 5B). The movement of neutrophils between the two sites did not occur to the same extent when Mm was injected further away from the tailfin wound (23–24th somite) and injection closer to the wound site (30th somite) caused early neutrophil movement to the infection site before the embryos could be mounted for microscopy; therefore, injection into the 26-27th somite was chosen as being optimal (Fig. 5B). Wound-naïve neutrophils were attracted to the infection site, but numbers remained steady between 0 and 110 mpc (minutes postconversion) (Fig. 5B). By 100 mpc, almost all wound-experienced neutrophils had been attracted away from the tailfin wound towards the infection site (Fig. 5C-F). These data demonstrate that the 'second hit' of infection was sufficient to overcome signalling that retains neutrophils at the initial tailfin wound site.

Hif-1α stabilisation retained neutrophils at infection at the expense of migration to a tailfin wound

Hypoxia signalling, via stabilisation of Hif-1α, has profound effects on neutrophil behaviours and antimicrobial activity [12,22,23]. We set out to understand whether Hif-1α stabilisation affected neutrophil behaviour in our comorbid models of infection and inflammation. We first stabilised Hif-1α in our simultaneous local infection and tailfin wound comorbid model to determine neutrophil migrations towards the two sites. Endogenous Hif-1α was stabilised pharmacologically using the hydroxylase inhibitors FG4592 and dimethyloxalylglycine (DMOG) [12] 4 h before infection with Mm into the 26–27th muscle somite. This was followed by immediate tailfin wound, and neutrophil numbers were counted at each site at 6 pw/I (Fig. 6A). The solvent control for both hydroxylase inhibitors (DMSO) caused no difference in neutrophil migration to infection and wound at 6 hpw/i compared to untreated larvae (Fig. 6B–F). Treatment with either FG5492 or DMOG caused significantly increased neutrophil migration to the infection site with fewer neutrophils migrating to the tailfin wound compared to DMSO controls (Fig. 6B–F). These findings were confirmed by genetic stabilisation of Hif-1α using dominant active Hif-1α (Fig. 6G–

I). These data suggest that neutrophils primed with Hif-1α are more sensitive to the local infection chemokine gradient at the expense of the more distant gradient emanating from the wound.

Hif-1α stabilisation delayed wound-experienced neutrophil migration to Mm infection

We have previously demonstrated, in a single tailfin wound model, that stabilisation of Hif-1α delays neutrophil reverse migration away from the wound [12]. However, here we show that a local Mm infection is able to attract neutrophils away from the tailfin wound prematurely (Fig. 5). We therefore hypothesised that Hif-1α would prevent wound-experienced neutrophils from exiting the injury site prematurely to migrate to a localised infection site. We tested this in our comorbid model where local infection was performed 4 h post-tailfin wound. Wound-naïve neutrophil attraction to the site of Mm infection was not altered by DA Hif-1α compared to phenol red (PR) controls (Fig. 7A,B). Infection was sufficient to attract wound-experienced neutrophils away from the wound prematurely, but neutrophils in DA Hif-1α embryos were significantly delayed in their migration towards localised Mm infection compared to PR controls (Fig. 7B,C). The migration speed of wound-experienced neutrophils was lower in the DA Hif-1α group compared to the PR group, largely due to their tighter association to the wound edge and less migration away (Fig. 7D). This decrease in migration speed was more marked in wound-experienced neutrophils that were successful in migrating away from the wound edge towards the Mm infection site (Fig. 7E). These neutrophils migrated to the infection site at two-thirds of the speed in DA Hif-1α embryos compared to the PR controls (Fig. 7E). Furthermore, they took a less direct route to the infection, with the meandering index of these neutrophils significantly lower in the DA Hif-1α group compared to PR controls (Fig. 7F). Neutrophils in Hif-1α-stabilised embryos therefore remain more sensitive to the

wound signalling gradient, even if successful in escaping the wound to a second hit of infection.

Taken together, these data indicate that wound-experienced neutrophils in Hif-1α-stabilised larvae remain more sensitive to the wound gradient and are less likely to migrate to the second-hit infection site compared to normal controls.

Mm burden was decreased by Hif-1α stabilisation, despite delayed resolution of neutrophilic inflammation

In the single model of Mm infection, we have previously shown that Hif-1α stabilisation reduced bacterial burden; a good therapeutic outcome [22]. However, in the single tailfin model, Hif-1α delayed neutrophil inflammation resolution away from the wound, a bad therapeutic outcome in diseases of chronic inflammation [12]. As infection and chronic inflammation are common attributes of comorbidities, we investigated whether the beneficial therapeutic outcome of Hif-1α stabilisation in systemic infection would be maintained in the presence of chronic inflammation.

We observed an increase in neutrophil recruitment to the tailfin wound after Mm infection (at 6 hpw) in PR controls (Fig. 8A,B), in keeping with the emergency haematopoietic effect of infection observed earlier (Fig. 1D). No effect of DA Hif-1α was observed on neutrophil recruitment compared to PR controls (Fig. 8B), consistent with previous observations in the single tailfin transection model [12]. Neutrophil numbers at the wound after resolution at 24 hpw were increased by DA Hif-1α compared to PR controls in the presence (Mm) or absence (PVP) of Mm infection (Fig. 8C), and the percentage resolution (6–24 hpw) was reduced by Hif-1α stabilisation compared to PR controls (Fig. 8D), indicating that Hif-1α stabilisation delays neutrophil inflammation resolution in the presence of systemic infection.

DA Hif-1α larvae had decreased bacterial burden compared to PR controls indicating that the protective
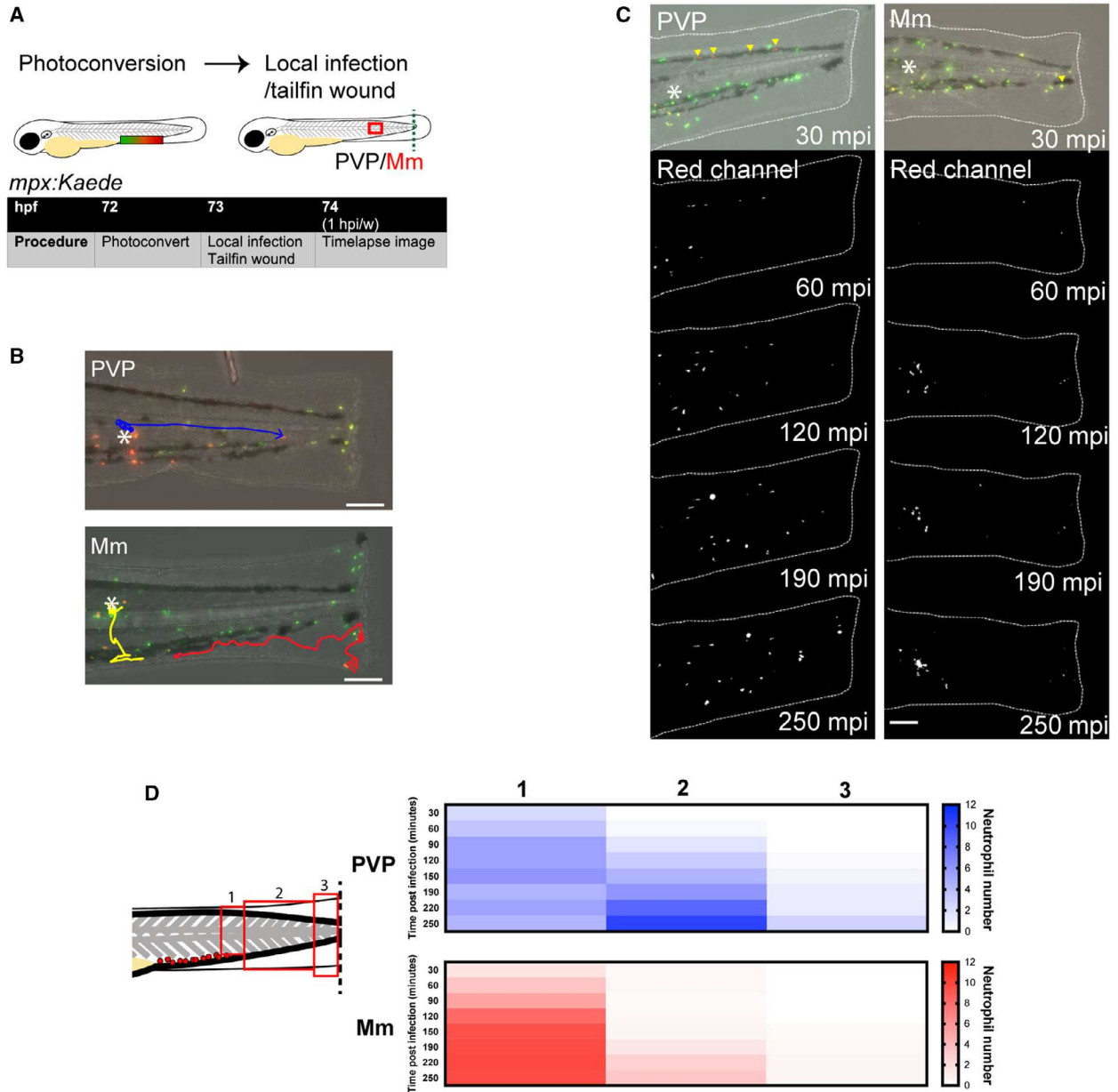
Fig. 3. Mm retains neutrophils at the somite infection site at the expense of migration to the tailfin wound. (A) Schematic of experiment for B–D, showing PC of neutrophils in the CHT of *mpx:Kaede* embryos. (B) Example fate-tracks of red neutrophils that were photoconverted in the CHT and migrated to either PVP or Mm infection in the somite over 4 hpi/w. Data shown are examples from two independent experiments with 10 fish per group. Scale bar = 100 μM. (C) Stereo-fluorescence micrographs of the location of red photoconverted neutrophils that originated in the CHT in PVP and Mm-infected larvae. Data shown are examples from two independent experiments with 10 fish per group. Scale bar = 100 μM. (D) Heatmap of location of red photoconverted neutrophils that originated in the CHT over time. Data shown are *n* = 5 embryos per group accumulated from two independent experiments.

effects of Hif-1α stabilisation remained, even in the presence of tailfin inflammation (Fig. 8E,F). This is despite our finding that an inflammatory process (tailfin wound) during systemic infection caused a marked

increase in infection levels in the absence of Hif-1α stabilisation (Fig. 8E,F). These results indicate that Hif-1α remains protective against Mm even when neutrophil inflammation resolution is delayed at the tailfin.
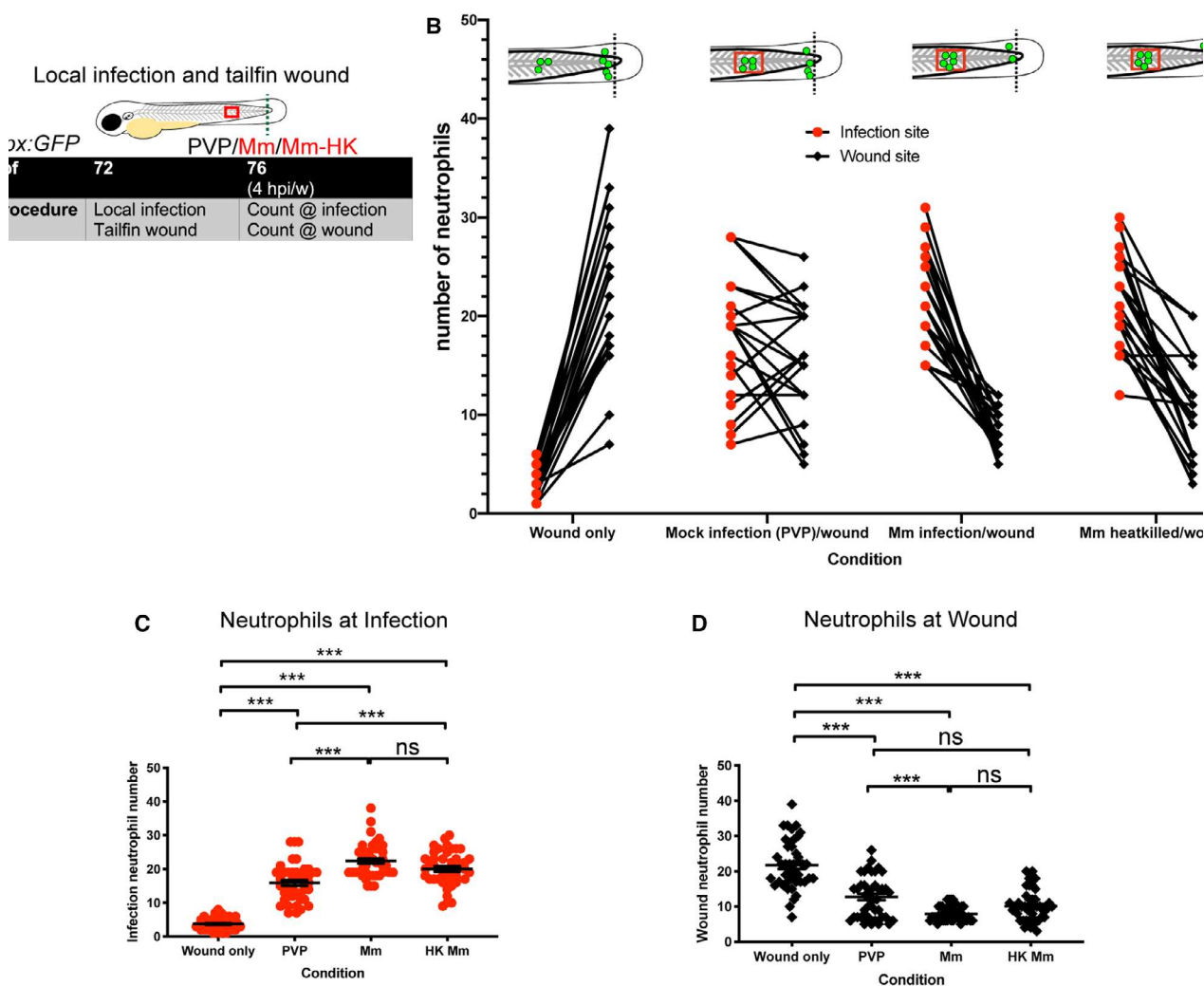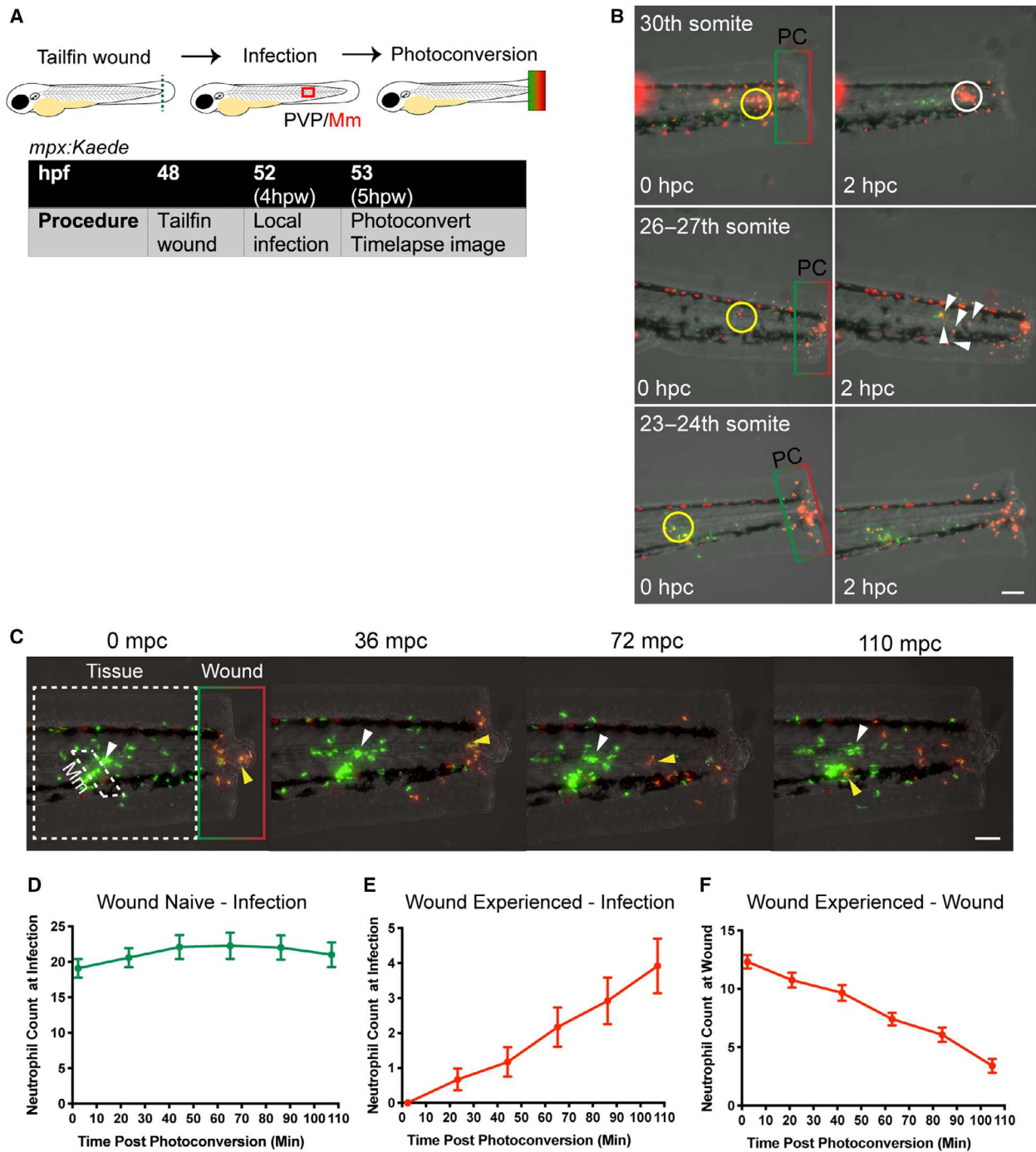
Fig. 4. HK Mm are sufficient for increased neutrophil recruitment to the infection site. (A) Schematic of experiment for B–D. (B) Number of neutrophils at site of infection and tailfin wound at 4 hpi/w in *mpx:GFP* embryos. The groups are Wound (tailfin wound alone), Mock infection (PVP)/wound (injection of PVP into the somite alongside a tailfin wound), Mm infection/wound (injection of Mm into the somite alongside a tailfin wound) and HK Mm infection/wound (injection of HK Mm into the somite alongside a tailfin wound). Individual embryos are represented as lines joining their respective infection and tailfin wound neutrophil numbers. Data shown are mean ± SEM, *n* = 21 representative of three independent experiments. (C) Neutrophil numbers at the site of infection at 4 hpi. Data shown are mean ± SEM, *n* = 42 representative of three independent experiments. Statistics were determined using an unpaired *t*-test. *P* values shown are as follows: ns = not significant and ***P < 0.001. (D) Neutrophil numbers at the site of tailfin wound at 4 hpi. Data shown are mean ± SEM, *n* = 42 representative of three independent experiments. Statistics were determined using an unpaired *t*-test. *P* values shown are as follows: ns = not significant and ***P < 0.001.

Discussion

With the emergence of antibiotic resistance, there is increasing interest to find host-derived factors that could act as therapeutic targets [2]. We have previously identified in zebrafish *in vivo* models of TB infection that targeting neutrophils is a potential mechanism to decrease infection burden via Hif-1α stabilisation [22]. Physiological hypoxia and Hif-1α stabilisation have

been demonstrated to have activating effects on neutrophils in a growing number of models, increasing their antimicrobial capabilities *in vitro*, *ex vivo* and *in vivo* [18,19]. These findings have been tempered by clinical observations that activated neutrophils are associated with chronic disease, leading to excess tissue damage and poor disease outcomes [11,23]. Patient studies address neutrophil behaviour at chronic stages

A

Tailfin wound → Infection → Photoconversion

PVP/Mm

mpx:Kaede

hpf	48	52 (4hpw)	53 (5hpw)
Procedure	Tailfin wound	Local infection	Photoconvert Timelapse image

B

30th somite — PC — 0 hpc / 2 hpc

26–27th somite — PC — 0 hpc / 2 hpc

23–24th somite — PC — 0 hpc / 2 hpc

C

0 mpc — Tissue — Wound — Mm / 36 mpc / 72 mpc / 110 mpc

D Wound Naive - Infection

Neutrophil Count at Infection vs Time Post Photoconversion (Min)

E Wound Experienced - Infection

Neutrophil Count at Infection vs Time Post Photoconversion (Min)

F Wound Experienced - Wound

Neutrophil Count at Wound vs Time Post Photoconversion (Min)

of disease by which time there is a cycle of neutrophil overactivation, degranulation, tissue damage and further recruitment. Targeting neutrophils at earlier disease stages has the potential to be highly beneficial before this chronic cycle begins, but potential effects on patients with TB and comorbid inflammatory conditions, such as COPD, remain unclear.

By combining zebrafish Mm infection and a tailfin wound to make a comorbid model, we have shown that Hif-1α stabilisation remains protective against Mm infection in the presence of comorbid inflammation. This was despite infection burden being increased by the presence of a tailfin wound in the wild-type situation. While the increase in infection alongside a

Fig. 5. Neutrophils preferentially migrated to a new infection stimulus rather than patrol the wound site. (A) Schematic of experiment for B–F. (B) Stereo-fluorescence micrographs of a tailfin transected *mpx:Kaede* embryo after either 30th somite, 26/27th somite, or 23–24 somite infection with Mm at 0 and 2hpi. The local infection site is shown by a yellow ring, and PC of wound neutrophils is shown by the box. With 30 somite injection red (wound-experienced) neutrophils have started migration to the infection site by the time the time lapse has been started and are almost all at the infection site by 2 hpi (white ring). The 26-27th somite infection does not start recruiting wound-experienced neutrophil by the time of the time lapse, but has done so after 2 hpi (white arrowheads). Infection into the 23rd–24th somite does not recruit any wound-experienced neutrophils over a 2-h time course. Representative example from *n* = 9 embryos per group from three independent experiments. Scale bar = 150 μM. (C) Stereo-fluorescence micrographs of a tailfin transected *mpx:Kaede* embryo after 26/27th somite infection with Mm. Wound-naïve neutrophils are green only, and those photoconverted at the wound at timepoint zero (wound-experienced) begin as red-only and regain GFP (therefore giving a yellow overlay) over the course of the time lapse as nascent Kaede fluorescent protein is made. Both wound-naïve (white arrowhead) and wound-experienced (yellow arrowhead) are recruited to the localised site of Mm infection before 110 mpc, even though the time lapse is begun at 5 hpw, a timepoint when neutrophils would normally still be recruited to the tailfin transection. Representative example from data shown in D-F, *n* = 12 embryos from three independent experiments. Scale bar = 100 μM. (D) Number of green, wound-naïve neutrophils at infection site over 1.5 hpi. Data shown are mean ± SEM, *n* = 12 embryos accumulated from three independent experiments. (E) Number of red, wound-experienced neutrophils at infection site over 1.5 hpi. Data shown are mean ± SEM, *n* = 12 embryos accumulated from three independent experiments. (F) Number of red, wound-experienced neutrophils at wound site over 1.5 hpi. Data shown are mean ± SEM, *n* = 12 embryos accumulated from three independent experiments.

wound may be due to neutrophils migrating to the tailfin wound, it may also be due to differences in neutrophil activation by wounding and Hif-1α. After both wounding and Hif-1α stabilisation, there is robust upregulation of pro-inflammatory signalling, for example increased Interleukin 1 beta in neutrophils [31,32], but with wounding neutrophil activation appears detrimental to infection control while with Hif-1α stabilisation this is host protective. Signs of Hif-1α stabilisation being detrimental to neutrophilic inflammation resolution were observed at the tailfin wound in the comorbid model where resolution of neutrophil inflammation was delayed. However, no other adverse effects were observed, consistent with findings from the single tailfin wound model [12]. These data indicate that stimulation of neutrophils by inflammation (wounding) and Hif-1α stabilisation is different and that if neutrophils are appropriately activated by Hif-1α, they could be highly beneficial to host infection control without damaging holistic effects.

We developed a local infection and tailfin wound comorbid model to investigate the effects of Hif-1α stabilisation on neutrophil migration to wound and infection sites simultaneously. We found that neutrophils dispersed between infection and wound sites, but when Hif-1α was stabilised, neutrophils seldom migrated beyond the local infection on to the tailfin wound. Conversely, Hif-1α stabilisation retained neutrophils at the tailfin wound when a second hit of infection was introduced, while in wild-type larvae infection caused premature migration away from the wound to the infection site. These data indicate that Hif-1α stabilisation causes increased sensitivity to wound or infection gradients, leading to retention of neutrophils and reduced ability of these cells to

respond to competing signals. Our previous findings have shown that Hif-1α stabilisation caused no effect on neutrophil recruitment to the tailfin wound in the single inflammation model; therefore, Hif-1α is unlikely to have effects on neutrophil recruitment signalling [12]. Taken together, these data indicate that recognition of 'retention signals' by neutrophils is sensitised by stabilised Hif-1α, keeping neutrophils at the wound or infection site and that there is an as yet unidentified molecular change in neutrophils in Hif-1α-stabilised embryos that alters their sensitivity to these tissue gradients. Likely candidates for Hif-1α targets include G protein-coupled receptors (GPCRs) that are involved in neutrophil migration (many chemokine receptors are GPCRs) and are regulated by Hif-1α in immune cells (eg CXCR1, CXCR2 or CXCR4) [33–37]. Cxcr1/2 have been implicated in retention of neutrophils at wounds, and we have recently demonstrated that decreasing Cxcr4 signalling causes premature reverse migration away from the tailfin wound [38].

Previous findings in a zebrafish model of tailfin infection followed by localised infection demonstrated that, during the reverse migration phase of neutrophil inflammation (> 12 hpw), wound-experienced neutrophils that are migrating away from the wound towards infection stimuli (*Staphylococcus aureus* and zymosan) display unaltered migration behaviour compared to nearest-neighbour-wound-naïve neutrophils [39]. In the absence of Hif-1α stabilisation, this appears to be the case in our Mm/wound comorbid model, with both wound-naïve and wound-experienced neutrophils equally able to respond to the secondary local infection. When Hif-1α is stabilised, differences in neutrophil migration behaviour become evident – wound-experienced neutrophils change behaviour and
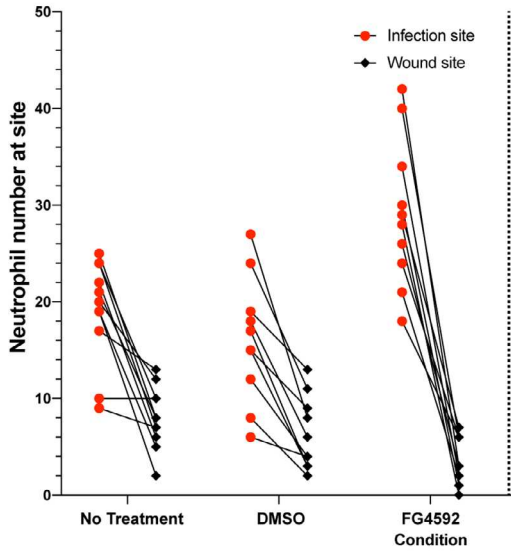
A Local infection and tailfin wound

mpx:GFP   PVP/Mm
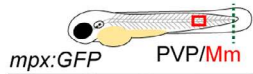
hpf	54	72	76 (4 hpi/w)
Procedure	DMSO/ FG4592	Local infection Tailfin wound	Count @ infection Count @ wound

hpf	54	72	76 (4 hpi/w)
Procedure	DMSO/ DMOG	Local infection Tailfin wound	Count @ infection Count @ wound

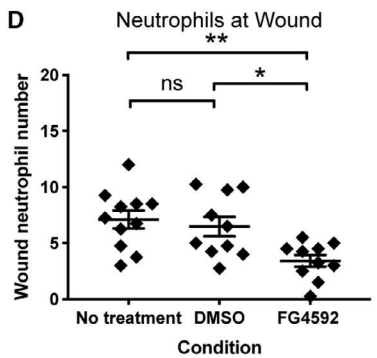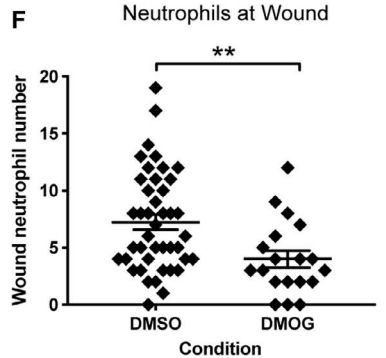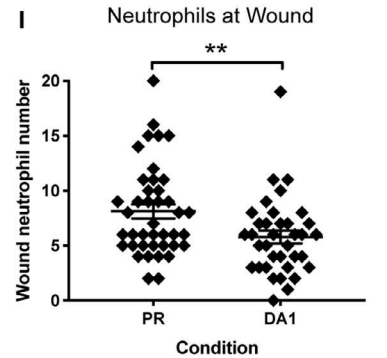| hpf	0-1	72	76 (4 hpi/w)
Procedure	PR/DA1 injection	Local infection Tailfin wound	Count @ infection Count @ wound
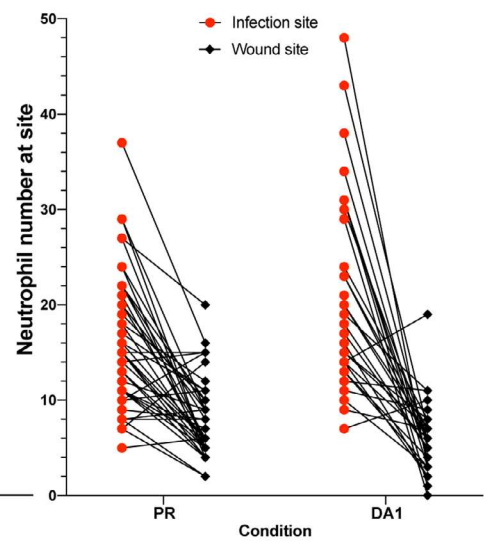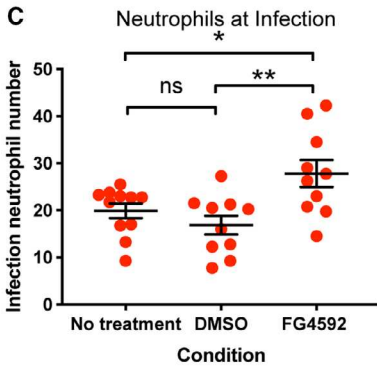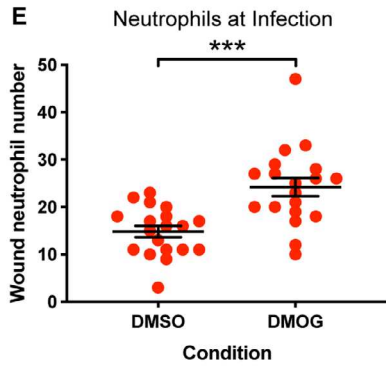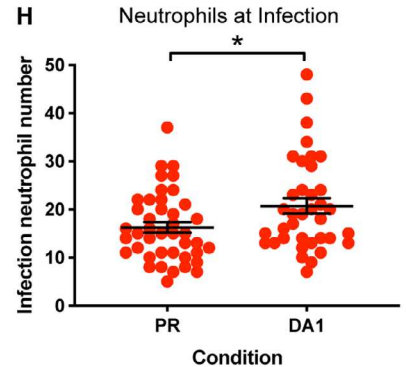
are slower to migrate to the second hit, while wound-naïve neutrophils migrate as normal. This indicates that neutrophils that have visited the wound may differ from those that have not in certain contexts (eg when Hif-1α is stabilised); however, the mechanisms behind these differences have yet to be determined.

Fig. 6. Hif-1α stabilisation increased neutrophil numbers at infection at the expense of those at the tailfin wound. (A) Schematic of experiment for B–F. (B) Number of neutrophils at site of infection and tailfin wound of *mpx:GFP* embryos at 4 hpi/w after Hif-1α stabilisation with FG4592 or DMOG with no treatment and DMSO controls. Data shown are mean ± SEM, *n* = 9–15 representative of three independent experiments. (C) Neutrophil numbers at the infection site at 4 hpi with DMSO and FG4592 treatment. Data shown are mean ± SEM, *n* = 10–11 representative of three independent experiments. Statistics were determined using one-way ANOVA (with Bonferroni's multiple comparisons test). *P* values shown are as follows: ns = not significant, *$P < 0.05$, and **$P < 0.01$. (D) Neutrophil numbers at the wound site at 4 hpi with DMSO and FG4592 treatment. Data shown are mean ± SEM, *n* = 10–11 representative of three independent experiments. Statistics were determined using one-way ANOVA (with Bonferroni's multiple comparisons test). *P* values shown are as follows: ns = not significant, *$P < 0.05$, and **$P < 0.01$. (E) Neutrophil numbers at the infection site at 4 hpi with DMSO and DMOG treatment. Data shown are mean ± SEM, *n* = 19 representative of three independent experiments. Statistics were determined using an unpaired *t*-test. *P* values shown are as follows: ***$P < 0.001$. (F) Neutrophil numbers at the wound site at 4 hpi with DMSO and DMOG treatment. Data shown are mean ± SEM, *n* = 19 representative of three independent experiments. Statistics were determined using an unpaired *t*-test. *P* values shown are as follows: **$P < 0.01$. (G) Number of neutrophils at site of infection and tailfin wound at 4 hpi/w after Hif-1α stabilisation with DA1 or PR controls. Data shown are mean ± SEM, *n* = 20–22 representative of three independent experiments. (H) Neutrophil numbers at the infection site at 4 hpi with PR and DA1. Data shown are mean ± SEM, *n* = 19 representative of three independent experiments. Statistics were determined using an unpaired *t*-test. *P* values shown are as follows: *$P < 0.05$. (I) Neutrophil numbers at the wound site at 4 hpi with PR and DA1 treatment. Data shown are mean ± SEM, *n* = 36–41 accumulated from three independent experiments. Statistics were determined using an unpaired *t*-test. *P* values shown are as follows: **$P < 0.01$.

Here, we kept as many aspects of each individual model as close as possible to those previously characterised in order to avoid setting up comorbid models with undefined individual characteristics that could potentially complicate interpretation [12,22]. Comorbidities can be incredibly complex, and further *in vivo* comorbid models are required to understand the full range of cellular and molecular mechanisms involved. Here, we only considered neutrophil migration towards infection and injury; however, macrophages also play important roles in the outcomes of wound and infection, as previously demonstrated in single-model zebrafish studies [10,28]. Future investigations into the role of macrophages in comorbid models may uncover novel mechanisms for macrophage migration and activity in wounds and infections when they occur together.

We used infection and sterile wounds as a comorbidity in this study; however, comorbidities can be more complex and further underlying conditions can affect both processes. A good example of this is diabetes, which suppresses the immune system, decreases wound healing and causes complex HIF dysregulation. Diabetes and hyperglycaemia can lead to localised tissue hypoxia due to links to obesity and changes in immunometabolism; however, hyperglycaemia also destabilises HIF-1α, which in part is responsible for the defective wound healing and infection responses [40,41]. Indeed, diabetes triples the chance of developing TB (WHO). The effects of HIF stabilisation in comorbidities such as diabetes and TB remain unclear.

As investigations of comorbidities continue to rise, we anticipate that comorbid models will increase in popularity, but with a plethora of possible conditions,

combinations and timings of stimuli available, care will be required to understand the relevance of these models to the research question asked.

Using comorbid models of infection and wounding, we have highlighted that comorbidity has a range of effects on neutrophil behaviour during infection that differ on the local tissue scale compared to the whole-organism, holistic, level. In our comorbid model, Hif-1α stabilisation remains host-protective effect while causing a delay in neutrophil inflammation resolution at a wound, properties that are consistent with the individual models [12,22]. Using a localised infection comorbid model, we show that Hif-1α stabilisation increases neutrophil retention at infection and tailfin wound sites *in vivo*. Our comorbid models suggest that, on a whole-organism level, neutrophil activation by Hif-1α stabilisation is able to reduce infection burden and remains a promising host-derived therapeutic strategy against multi-drug-resistant TB.

Materials and methods

Zebrafish husbandry

All the zebrafish used in this project were raised in the University of Sheffield Home Office approved aquarium and were kept under standard protocols as previously outlined [42]. Adult zebrafish were kept in tanks of no more than 40 adult fish and experience a 14-h light and 10-h dark cycle. A recirculating water supply is maintained, and the temperature of the water is kept at 28 °C. Embryos for this study were generated by in-crossing *TgBAC(mpx:Gal4.VP16);Tg(UAS:Kaede)i222* (shortened to *mpx:Kaede*) or *Tg(mpx:GFP)i114* (shortened to *mpx:GFP*) [27,43].
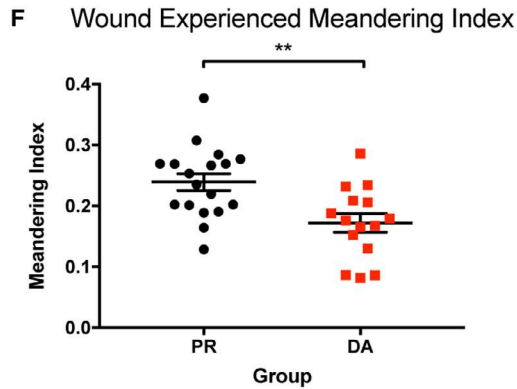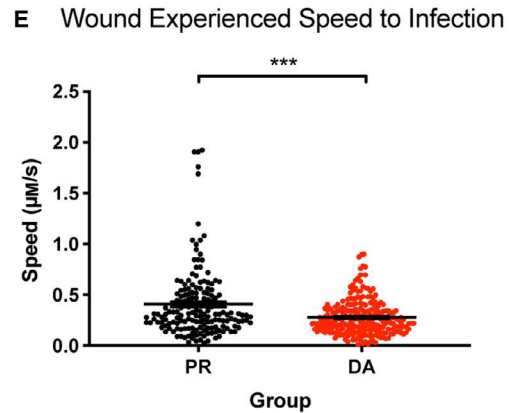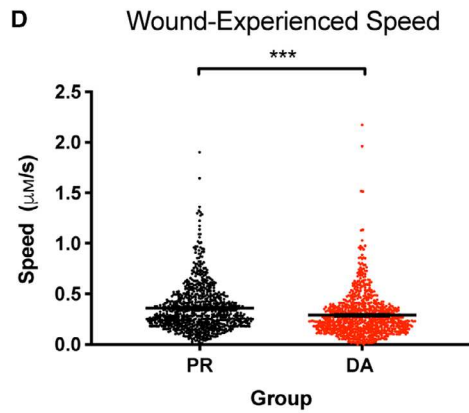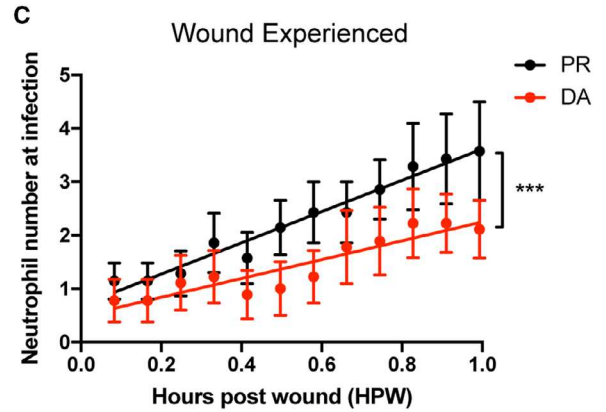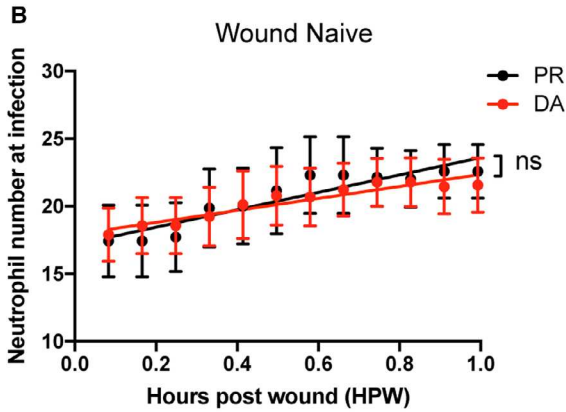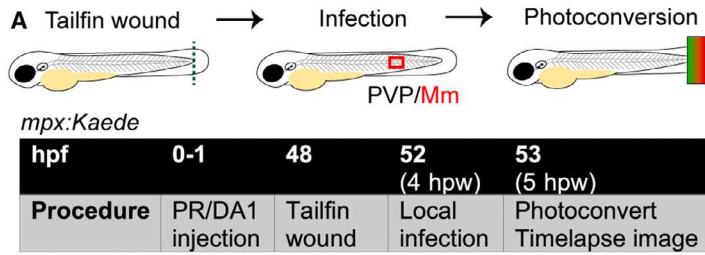
Fig. 7. Stabilisation of Hif-1α delayed the migration of wound-experienced neutrophils to a local site of Mm infection. (A) Schematic of experiment for B-F. (B) Number of green, wound-naïve neutrophils at infection site over 1 hpw in *mpx:Kaede* embryos. Groups shown are DA Hif-1α (DA, red points) and PR controls (black points). Data shown are mean ± SEM, $n = 7–9$ embryos accumulated from three independent experiments. Line of best fit shown is calculated by linear regression. *P* value shown is for the difference between the two slopes. *P* values shown are as follows: ns = not significant. (C) Number of red, wound-experienced neutrophils at infection site over 1 hpw. Groups shown are DA Hif-1α (DA, red points) and PR controls (black points). Data shown are mean ± SEM, $n = 7–9$ embryos accumulated from three independent experiments. Line of best fit shown is calculated by linear regression. *P* value shown is for the difference between the two slopes. *P* values shown are as follows: ***$P < 0.001$. (D) Speed of red, wound-experienced neutrophil movement at the wound site. Groups shown are DA Hif-1α (DA) and PR controls. Data shown are mean ± SEM, $n = 5–6$ embryos accumulated from three independent experiments. Statistics were determined using an unpaired *t*-test. *P* values shown are as follows: ***$P < 0.001$. (E) Speed of red, wound-experienced neutrophils migrating from the wound site to the infection site. Groups shown are DA Hif-1α (DA) and PR controls. Data shown are mean ± SEM, $n = 5–6$ embryos accumulated from three independent experiments. Statistics were determined using an unpaired *t*-test. *P* values shown are as follows: ***$P < 0.001$. (F) Meandering index of red, wound-experienced neutrophils migrating from the wound site to the infection site. Groups shown are DA Hif-1α (DA) and PR controls. Data shown are mean ± SEM, $n = 15–18$ embryos accumulated from two independent experiments. Statistics were determined using an unpaired *t*-test. *P* values shown are as follows: **$P < 0.01$. Scale bars = 500 μM.

Ethics

All procedures over the course of this project were performed on embryos that were less than 5.2 dpf and were therefore considered outside of the Animals (Scientific Procedures) Act. Procedures were carried out to standards set by the UK Home Office on the Project Licence P1A4A7A5E held by S. Renshaw at the University of Sheffield.

Tailfin transection

For all experiments, larval tailfins were transected at 48 hpf as previously described [12]. Kaede-expressing wound neutrophils were photoconverted at 4 hpw using a SOLA light engine white light LED (Lumencor, Beaverton, OR, USA) through DAPI filters on a Leica DMi8 inverted widefield microscope (Leica Microsystems (UK), Milton Keynes, UK). Time-lapse microscopy was performed using a Leica DMi8 inverted widefield microscope (Leica Microsystems) using a HC FL PLAB 10×/0.40 lens and captured using a Hamamatsu ORCA-Flash 4.0 camera (Hamamatsu, Hamamatsu-City, Japan). Neutrophil counts were performed with the investigator blinded to the experimental group on a Leica MZ10 F Stereomicroscope with fluorescence, with changes in focus and magnification allowing optical resolution of individual cells (Leica Microsystems).

Mycobacterium marinum infection

Mycobacterium marinum infection experiments were performed using *M. marinum* M (ATCC #BAA-535), containing a psMT3-mCherry or psMT3 mCrimson vector [44]. Injection inoculum was prepared from an overnight liquid culture in the log phase of growth resuspended in 2% PVP40 solution (CalBiochem/Merck KGaA, Darmstadt, Germany) as previously described [22]. For HK experiments, Mm were incubated at 80 °C for 30 min as previously described [45].

For systemic infection, 150–200 colony-forming units (CFU) were injected into the caudal vein at 28–30 hpf, as previously described [46].

For localised somite infection, fish were anaesthetised in 0.168 mg·mL^{-1} Tricaine (Sigma-Aldrich/Merck KGaA, Darmstadt, Germany) and were microinjected with 500CFU of Mm in the 26-27th somite [39].

Hif-1α stabilisation

Embryos were injected with dominant active *hif-1αb* (ZFIN: hif1ab) variant RNA at the one-cell stage as previously described [12,47]. PR (Sigma-Aldrich) was used as a vehicle control.

Hif-1α was stabilised pharmacologically using hydroxylase inhibitors FG4592, 5 μM or DMOG, 100 μM, with DMSO control.

Bacterial pixel count

Infected zebrafish larvae were imaged at 4 dpi on an inverted Leica DMi8 with a 2.5× objective lens. Brightfield and fluorescent images were captured using a Hamamatsu OrcaV4 camera. Bacterial burden was assessed using dedicated pixel counting software as previously described [22,45].

Image and Statistical analysis

Microscopy data were analysed using Leica LASX (Leica Microsystems) and IMAGEJ software (U. S. National Institutes of Health, Bethesda, MD, USA). Meandering index was calculated by dividing the shortest possible path from start to endpoint by the total distance travelled by the neutrophil over the time period. Therefore, a neutrophil
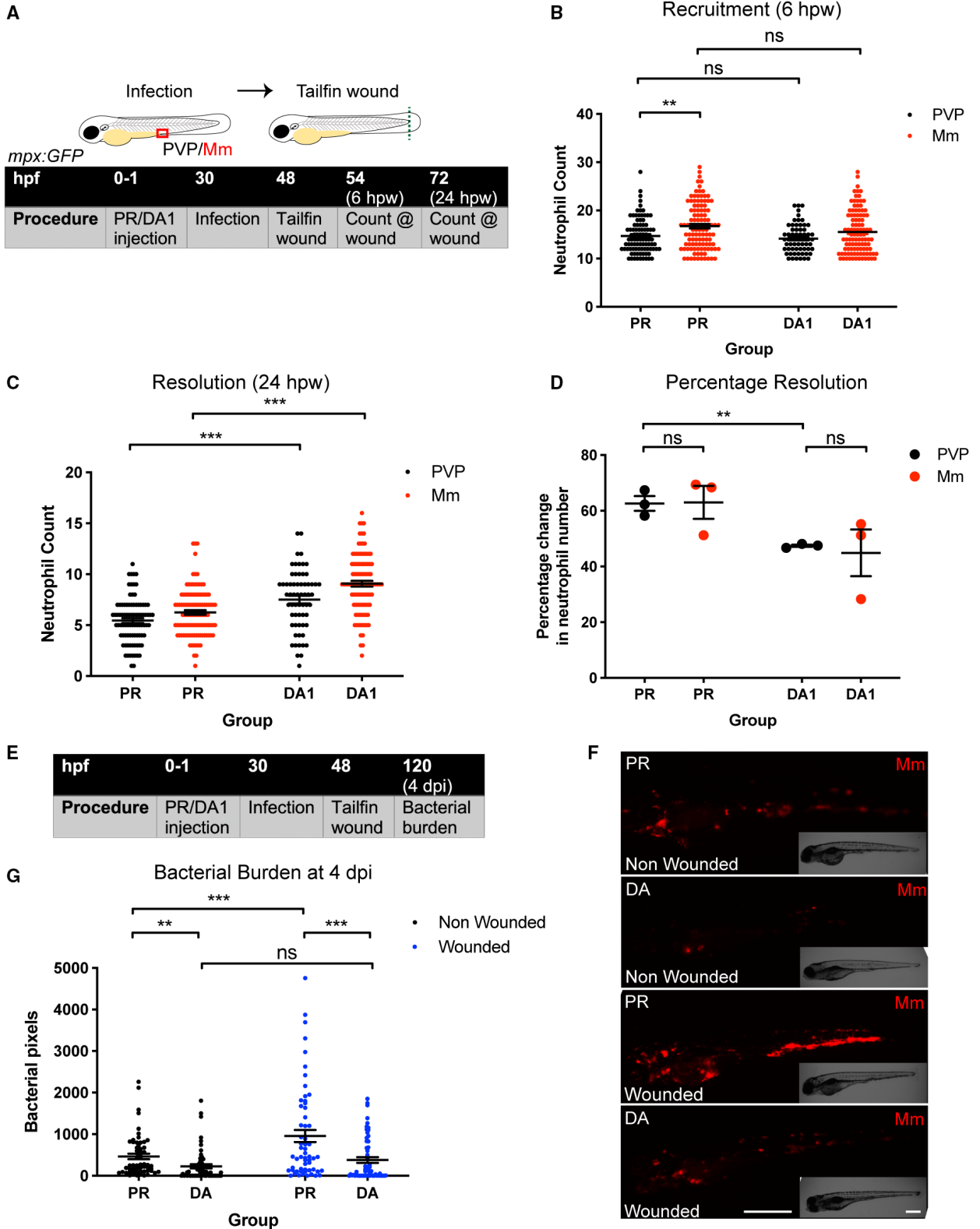
Fig. 8. Mm burden was decreased by Hif-1α stabilisation, despite delayed resolution of neutrophilic inflammation. (A) Schematic of experiment for B-D. (B) Neutrophil numbers recruited to the tailfin wound at 6 hpw in *mpx:GFP* embryos. Groups are PR and DA Hif-1α (DA) injected at 30 hpf with PVP or Mm. Data shown are mean ± SEM, *n* = 62–111 accumulated from three independent experiments. Statistics were determined using one-way ANOVA (with Bonferroni's multiple comparisons test). *P* values shown are as follows: ns = not significant and **$P < 0.01$. (C) Neutrophil numbers at the tailfin wound at 24 hpw. Groups are PR and DA Hif-1α (DA) injected at 30 hpf with PVP or Mm. Data shown are mean ± SEM, *n* = 62–111 accumulated from three independent experiments. Statistics were determined using one-way ANOVA (with Bonferroni's multiple comparisons test). *P* values shown are as follows: ***$P < 0.001$. (D) Percentage resolution of neutrophil inflammation (between 6 and 24 hpw). Groups are PR and DA Hif-1α (DA) injected at 30 hpf with PVP or Mm. Data shown are mean ± SEM, *n* = 62–111 accumulated from three independent experiments. Statistics were determined using one-way ANOVA (with Bonferroni's multiple comparisons test). *P* values shown are as follows: ns = not significant and **$P < 0.01$. (E) Schematic of experiment for G-F. (F) Stereo-fluorescence micrographs of Mm mCherry-infected 4 dpi larvae after injection with DA Hif-1α (DA1) and PR as a negative control and either wounded at 48 hpf or nonwounded in *mpx:GFP* embryos. Representative images from data shown in G, with *n* = 58 accumulated from three independent experiments. (G) Bacterial burden of larvae shown in (F). Data shown are mean ± SEM, *n* = 58 accumulated from three independent experiments. Statistics were determined using one-way ANOVA (with Bonferroni's multiple comparisons test). *P* values shown are as follows: ns = not significant, **$P < 0.01$, and ***$P < 0.001$.

travelling in a straight line would have a meandering index of 1 and a neutrophil deviating from the shortest path a meandering index of < 1. All data shown are mean with SEM (PRISM 8.0; GraphPad Software, San Diego, CA, USA) with statistics determined using *t*-tests for comparisons between two groups and one-way ANOVA (with Bonferroni post-test adjustment) for other data. *P* values shown are as follows: *$P < 0.05$, **$P < 0.01$, and ***$P < 0.001$.

Acknowledgements

Conflict of interest

The authors declare no conflict of interest.

Author contributions

YS, AM, EJW and PME conceived and designed the experiments. YS, AM, EJW, AL and PME performed the experiments. YS, AM, EJW and PME analysed the data. PME wrote the manuscript.

References

1 World Health Organisation (2018) Global Health TB Report.

2 Zumla A, Rao M, Parida SK, Keshavjee S, Cassell G, Wallis R, Axelsson-Robertsson R, Doherty M, Andersson J & Maeurer MJ (2015) Inflammation and tuberculosis: host-directed therapies. *J Intern Med* **277**, 373–387.

3 Lowe DM, Redford PS, Wilkinson RJ, O'Garra A & Martineau AR (2012) Neutrophils in tuberculosis: friend or foe? *Trends Immunol* **33**, 14–25.

4 De Oliveira S, Rosowski EE & Huttenlocher A (2016) Neutrophil migration in infection and wound repair: going forward in reverse. *Nat Rev Immunol* **16**, 378–391.

5 Tan RST, Ho B, Leung BP & Ding JL (2014) TLR cross-talk confers specificity to innate immunity. *Int Rev Immunol* **33**, 443–453.

6 Yang CT, Cambier CJ, Davis JM, Hall CJ, Crosier PS & Ramakrishnan L (2012) Neutrophils exert protection in the early tuberculous granuloma by oxidative killing of mycobacteria phagocytosed from infected macrophages. *Cell Host Microbe* **12**, 301–312.

7 Pedrosa J, Saunders BM, Appelberg R, Orme IM, Silva MT & Cooper AM (2000) Neutrophils play a protective nonphagocytic role in systemic *Mycobacterium tuberculosis* infection of mice. *Infect Immun* **68**, 577–583.

8 Fulton SA, Reba SM, Martin TD & Boom WH (2002) Neutrophil-mediated mycobacteriocidal immunity in the lung during *Mycobacterium bovis* BCG infection in C57BL/6 mice. *Infect Immun* **70**, 5322–5327.

9 Hoenderdos K & Condliffe A (2013) The neutrophil in chronic obstructive pulmonary disease. *Am J Respir Cell Mol Biol* **48**, 531–539.

10 Loynes CA, Martin JS, Robertson A, Trushell DM, Ingham PW, Whyte MK & Renshaw SA (2010) Pivotal advance: pharmacological manipulation of inflammation resolution during spontaneously resolving tissue neutrophilia in the zebrafish. *J Leukoc Biol* **87**, 203–212.

11 Thompson AAR, Elks PM, Marriott HM, Eamsamarng S, Higgins KR, Lewis A, Williams L, Parmar S, Shaw G, McGrath EE *et al.* (2014) Hypoxia-inducible factor

2a regulates key neutrophil functions in humans, mice, and zebrafish. *Blood* **123**, 366–376.

12 Elks PM, Van Eeden FJ, Dixon G, Wang X, Reyes-Aldasoro CC, Ingham PW, Whyte MKB, Walmsley SR & Renshaw SA (2011) Activation of hypoxia-inducible factor-1α (hif-1α) delays inflammation resolution by reducing neutrophil apoptosis and reverse migration in a zebrafish inflammation model. *Blood* **118**, 712–722.

13 Genschmer KR, Russell DW, Lal C, Szul T, Bratcher PE, Noerager BD, Abdul Roda M, Xu X, Rezonzew G, Viera L *et al.* (2019) Activated PMN exosomes: pathogenic entities causing matrix destruction and disease in the lung. *Cell* **176**, 113–126.

14 Uddin M, Watz H, Malmgren A & Pedersen F (2019) NETopethic inflammation in chronic obstructive pulmonary disease and severe asthma. *Front Immunol* **10**, 47.

15 Bates M, Marais BJ & Zumla A (2015) Tuberculosis comorbidity with communicable and noncommunicable diseases. *Cold Spring Harbor Perspect Med* **5**, a017889.

16 Sbrana E, Grise J, Stout C & Aronson J (2011) Co-morbidities associated with tuberculosis in an autopsy case series. *Tuberculosis* **91**, S38–S42.

17 Hunter P (2012) The inflammation theory of disease. the growing realization that chronic inflammation is crucial in many diseases opens new avenues for treatment. *EMBO Rep* **13**, 968–970.

18 Peyssonnaux C, Datta V, Cramer T, Doedens A, Theodorakis EA, Gallo RL, Hurtado-Ziola N, Nizet V & Johnson RS (2005) HIF-1alpha expression regulates the bactericidal capacity of phagocytes. *J Clin Invest* **115**, 1806–1815.

19 Nizet V & Johnson RS (2009) Interdependence of hypoxic and innate immune responses. *Nat Rev Immunol* **9**, 609–617.

20 Cramer T, Yamanishi Y, Clausen BE, Förster I, Pawlinski R, Mackman N, Haase VH, Jaenisch R, Corr M, Nizet V *et al.* (2003) HIF-1α is essential for myeloid cell-mediated inflammation. *Cell* **112**, 645–657.

21 Elks PM, Renshaw SA, Meijer AH, Walmsley SR & van Eeden FJ (2015) Exploring the HIFs, buts and maybes of hypoxia signalling in disease: lessons from zebrafish models. *Dis Model Mech* **8**, 1349–1360.

22 Elks PM, Brizee S, van der Vaart M, Walmsley SR, van Eeden FJ, Renshaw SA & Meijer AH (2013) PLOS pathogens: hypoxia inducible factor signaling modulates susceptibility to mycobacterial infection via a nitric oxide dependent mechanism. *PLoS Pathog* **9**, e1003789.

23 Walmsley SR, Print C, Farahi N, Peyssonnaux C, Johnson RS, Cramer T, Sobolewski A, Condliffe AM, Cowburn AS, Johnson N *et al.* (2005) Hypoxia-induced neutrophil survival is mediated by HIF-1alpha-dependent NF-kappaB Activity. *J Exp Med* **20**, 105–115.

24 Renshaw SA & Trede NS (2012) A model 450 million years in the making: zebrafish and vertebrate immunity. *Dis Model Mech* **5**, 38–47.

25 Meijer AH (2016) Protection and pathology in TB: learning from the zebrafish model. *Semin Immunopathol* **38**, 261–273.

26 Mathias JR, Perrin BJ, Liu T-X, Kanki J, Look AT & Huttenlocher A (2006) Resolution of inflammation by retrograde chemotaxis of neutrophils in transgenic zebrafish. *J Leukoc Biol* **80**, 1281–1288.

27 Renshaw SA, Loynes CA, Trushell DM, Elworthy S, Ingham PW & Whyte MK (2006) A transgenic zebrafish model of neutrophilic inflammation. *Blood* **108**, 3976–3978.

28 Davis JM, Clay H, Lewis JL, Ghori N, Herbomel P & Ramakrishnan L (2002) Real-time visualization of mycobacterium-macrophage interactions leading to initiation of granuloma formation in zebrafish embryos. *Immunity* **17**, 693–702.

29 Hall CJ, Flores MV, Oehlers SH, Sanderson LE, Lam EY, Crosier KE & Crosier PS (2012) Infection-responsive expansion of the hematopoietic stem and progenitor cell compartment in zebrafish is dependent upon inducible nitric oxide. *Cell Stem Cell* **10**, 198–209.

30 Holmes GR, Dixon G, Anderson SR, Reyes-Aldasoro CC, Elks PM, Billings SA, Whyte MKB, Kadirkamanathan V & Renshaw SA (2012) Drift-diffusion analysis of neutrophil migration during inflammation resolution in a zebrafish model. *Adv Hematol* **2012**, 1–8.

31 Ogryzko NV, Hoggett EE, Solaymani-Kohal S, Tazzyman S, Chico TJA, Renshaw SA & Wilson HL (2014) Zebrafish tissue injury causes upregulation of interleukin-1 and caspase-dependent amplification of the inflammatory response. *Dis Model Mech* **7**, 259–264.

32 Ogryzko NV, Lewis A, Wilson HL, Meijer AH, Renshaw SA & Elks PM (2019) Hif-1α–induced expression of Il-1β protects against mycobacterial infection in zebrafish. *J Immunol* **202**, 494–502.

33 Wang X, Li C, Chen Y, Hao Y, Zhou W, Chen C & Yu Z (2008) Hypoxia enhances CXCR4 expression favoring microglia migration via HIF-1α activation. *Biochem Biophys Res Commun* **371**, 283–288.

34 Guan G, Zhang Y, Lu Y, Liu L, Shi D, Wen Y, Yang L, Ma Q, Liu T, Zhu X *et al.* (2015) The HIF-1alpha/CXCR4 pathway supports hypoxia-induced metastasis of human osteosarcoma cells. *Cancer Lett* **357**, 254–264.

35 Walters KB, Green JM, Surfus JC, Yoo SK & Huttenlocher A (2010) Live imaging of neutrophil motility in a zebrafish model of WHIM syndrome. *Blood* **116**, 2803–2811.

36 Oh YS, Kim HY, Song IC, Yun HJ, Jo DY, Kim S & Lee HJ (2012) Hypoxia induces CXCR4 expression and biological activity in gastric cancer cells through

activation of hypoxia-inducible factor-1alpha. *Oncol Rep* **28**, 2239–2246.

37 Yamada M, Kubo H, Kobayashi S, Ishizawa K, He M, Suzuki T, Fujino N, Kunishima H, Hatta M, Nishimaki K *et al.* (2011) The increase in surface CXCR4 expression on lung extravascular neutrophils and its effects on neutrophils during endotoxin-induced lung injury. *Cell Mol Immunol* **8**, 305–314.

38 Isles HM, Herman KD, Robertson AL, Loynes CA, Prince LR, Elks PM & Renshaw SA (2019) The CXCL12/CXCR4 signaling axis retains neutrophils at inflammatory sites in zebrafish. *Front Immunol* **10**, 1784.

39 Ellett F, Elks PM, Robertson AL, Ogryzko NV & Renshaw SA (2015) Defining the phenotype of neutrophils following reverse migration in zebrafish. *J Leukocyte Biol* **98**, 975–981.

40 Botusan IR, Sunkari VG, Savu O, Catrina AI, Grünler J, Lindberg S, Pereira T, Ylä-Herttuala S, Poellinger L, Brismar K *et al.* (2008) Stabilization of HIF-1α is critical to improve wound healing in diabetic mice. *Proc Natl Acad Sci USA* **105** 19426–19431.

41 Lee YS, Wollam J & Olefsky JM (2018) An integrated view of immunometabolism. *Cell* **172**, 22–40.

42 Nüsslein-Volhard C & Dham R (2002) Zebrafish: A Practical Approach. Oxford University Press, New York, NY.

43 Robertson AL, Holmes GR, Bojarczuk AN, Burgon J, Loynes CA, Chimen M, Sawtell AK, Hamza B, Willson J, Walmsley SR *et al.* (2014) A zebrafish compound screen reveals modulation of neutrophil reverse migration as an anti-inflammatory mechanism. *Sci Translat Med* **6**, 225ra29.

44 van der Sar AM, Spaink HP, Zakrzewska A, Bitter W & Meijer AH (2009) Specificity of the zebrafish host transcriptome response to acute and chronic mycobacterial infection and the role of innate and adaptive immune components. *Mol Immunol* **46**, 2317–2332.

45 Elks PM, van der Vaart M, van Hensbergen V, Schutz E, Redd MJ, Murayama E, Spaink HP & Meijer AH (2014) Mycobacteria counteract a TLR-mediated nitrosative defense mechanism in a zebrafish infection model. *PLoS One* **9**, e100928.

46 Benard EL, van der Sar AM, Ellett F, Lieschke GJ, Spaink HP & Meijer AH (2012) Infection of zebrafish embryos with intracellular bacterial pathogens. *J Vis Exp* **61**, e3781.

47 Santhakumar K, Judson EC, Elks PM, McKee S, Elworthy S, Van Rooijen E, Walmsley SS, Renshaw SA, Cross SS & Van Eeden FJM (2012) A zebrafish model to study and therapeutically manipulate hypoxia signaling in tumorigenesis. *Cancer Res* **72**, 4017–4027.